Material Behaviour and Influence of Ceramics for Application in a Sensor Housing under High Temperature Load

Fabian Kohler, Jonas Krämer, Jürgen Wilde, University of Freiburg – IMTEK, Department of Microsystems Engineering, Freiburg, Germany, fabian.kohler@imtek.uni-freiburg.de
Michal Schulz, Holger Fritze, Clausthal University of Technology, Institute of Energy Research and Physical Technologies, Goslar, Germany.

Abstract

This paper presents a suitable material combination for sensor housings for temperatures up to 1000 °C. The focus is on the combination of different ceramic materials in the assembly. The thermal expansion coefficients must be matched to each other. The sensor housing, the carrier substrate and the electrical conductor paths must also perform reliably in the high-temperature range.
The connection between the housing cap and substrate is made with a high-temperature glass solder. The housing and substrate connection is thermally cycled between 200 °C and 1000 °C and tested for shear strength. The results are compared to simulation. Furthermore, the connection between glass solder and sapphire is verified by metallographic cross-sections. Also, X-ray diffraction is used to determine the joint quality.
The CTGS ($Ca_3TaGa_3Si_2O_{14}$) sensor element is bonded with glass solder as well. The two-sided mounting of the sensor will lead to mechanical stresses in the sensor material. Therefore, the displacement of the sensor element in the ceramic spacer under temperature load has to be monitored using optical measurement technology. The hardness of the CTGS sensor material is determined by hardness testing according to Vickers. The resistance to crack propagation is calculated from these tests.
The mechanical temperature-dependent material parameters are additionally entered into a FE-simulation in order to verify the simulative alignment of the experiments.
As a result, temperature-dependent material properties and a simulation model of the sensor package up to 1000 °C are available. The temperature sensor based on the housed BAW resonator was already functionally tested.

1 Introduction and Objectives

Sensors based on piezoelectric mono-crystals enable operation at extreme temperatures. The measured property is the resonance frequency which allows the development of sensors for temperature, pressure and other physical quantities. Langasite belongs to a larger family of high-temperature stable piezoelectric crystals that provide stable operation beyond the limits of proven quartz or piezoelectric ceramics [1-3]. CTGS ($Ca_3TaGa_3Si_2O_{14}$) is a member of the Langasite family with the general chemical formula $A_3BC_3D_2O_{14}$. In this work, CTGS is used as sensor material. In addition to the sensor element, the assembly and interconnection technology must also be able to withstand high temperatures.

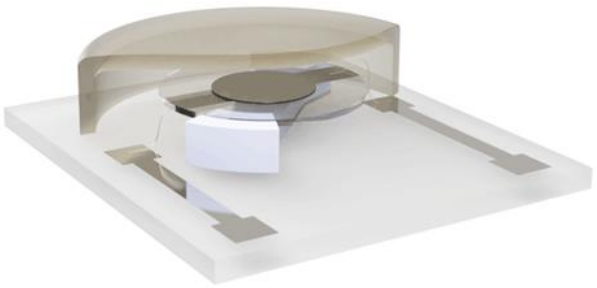

Figure 1: Assembly of the sensor setup. Sensor housing including resonator on support structure as well as platinum tracks and wire bonds for signal transmission [6,7].

A challenge in the temperature range up to 1000 °C is the selection of the right material combination. The materials and associated parameters such as the coefficient of expansion should be matched to each other that, so there is no excessive mechanical stress or material failure.
Apart from that a stable and tight sensor housing provides protection against strongly oxidising or reducing atmospheres.
The sensor structure shown in figure 1 represents various material combinations. The concept includes a sapphire base plate, a housing lid and a spacer made from aluminium oxide (Al_2O_3). The substrate is metallised with platinum conductor tracks, manufactured in thick-film technology. The ceramic components are fused with glass solder, which consists of a mixture of different oxides.
The wide range of the reported CTE-values of sapphire can be explained by the temperature range from 20 °C up to 1000 °C. The values of platinum, glass solder and aluminium oxide are for the temperature range from 20 °C to 300 °C. In addition to the temperature dependence of the CTE-values in the temperature range up to 1000 °C must be taken into account. The CTE value of the sensor element mentioned here refers to an own dilatometer measurement in the temperature range from 300 °C to 1000 °C.

ISBN 978-3-8007-5835-7

Table 1: Coefficient of thermal expansion of the materials used according to literature and manufacturer's specifications.

Packaging element	Material	CTE in ppm/K (source of data)
Substrate	Sapphire	6.6 – 9.0 (Dobrovinskaya et al, 2009)
Metallisation, wire bonds	Platinum	9.0 (Heraeus)
Glass solder	Mixture of oxides	8.4 (Schott)
Housing lid	Aluminium oxide	8.5 (C-technology)
Sensor element	$Ca_3TaGa_3Si_2O_{14}$	8,2 (own measurement)

In this work, sapphire (single-crystalline Al_2O_3), is used as the substrate material with a thickness of 650 µm. The cap and spacer are manufactured with an ultrasonic milling machine and are made of multi-crystalline alumina with a purity of 96 %.
The G18-385 glass solder is a reactive joining glass for high-temperature applications. The material composition is listed in Table 2. The multi-material mix should be in a semi-crystalline state after the firing process with a maximum temperature of 950 °C (10 min) and a crystallisation phase of 850 °C (120 min).

Table 2: Composition of the glass solder ingredients G018-385.

Material	Al_2O_3	B_2O_3	CaO	MgO	SiO_2	YO	ZrO_2
Weight-%	1-10	1-10	10-50	1-10	10-50	10-50	1-10

2 Technology and Materials

2.1 Dilatometer measurement

A dilatometer is a precision instrument for the measurement of dimensional changes in a material as a function of temperature. The dilatometer used in this work is a DIL 402 C from the company Netzsch with a temperature range from room temperature to a maximum of 1600 °C. In the measurements shown here, the samples are exposed to a maximum temperature of 1050 °C. The heating rate used for the measurement is 10 K/min.

2.2 Micro hardness testing of the senor material

The experiments to determine the microhardness of the sensor material were carried out on a testing machine from Anton Paar UNHT. The hardness of the 300 µm CTGS resonators is measured using the Vickers method with a test load of 200 mN (equivalent to HV 0.02). 9 indentations are measured to determine the hardness. The platinum electrode of the sensor element is removed by grinding with a SiC abrasive paper P2500. The evaluation is based on the measurement evaluation of the indentations under the microscope. If the indentations are placed too close to each other, they will influence themselves. Therefore, a distance of 100 µm was chosen here.
An additional important parameter, the fracture toughness K_{1c}, can be calculated using the formula from Anstis et al. [4].

$$K_{1c} = 0{,}016\left(\frac{E}{H}\right)^{0.5}\left(\frac{P}{c^{1.5}}\right) \quad (1)$$

P is the indentation force, c is the crack length, E is the Young's modulus and H is the hardness, where hardness is defined as a quantity with the unit GPa. This value can be converted from the measured Vickers hardness with the factor 0.009807 into a hardness value with the unit GPa.
The fracture toughness K_{1C}, is the critical stress intensity applied to the crack tip when unstable crack growth begins. The effective Young's modulus can be determined by the method of Oliver and Pharr. This method is based on Hertz' theory for elastic contact, which states that the stiffness S of the contact between two elastic spheres. Direct measurement of S (stiffness) and A_c (projected area of contact) allows E_r to be evaluated from equation 2 (Oliver & Pharr).

$$E_r = \left(\frac{\sqrt{\pi}}{2}\right)\left(\frac{S}{\sqrt{A_c}}\right) \quad (2)$$

2.3 XRD measurement

In an XRD measurement, the sample is illuminated with monochromatic X-ray radiation. Copper K-α radiation with a wavelength of $1.54 \cdot 10^{-10}$ m is used for the measurement.
The X-ray diffractometer used is an X'Pert³ with a PIXcel3D detector from Malvern Panalytical.
In this work, both single-crystal sapphire and glass solder are examined.

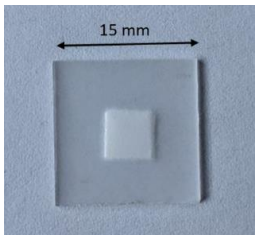

Figure 2: Fired glass solder surface (G018-385) on sapphire substrate.

2.4 Optical deformation measurement

For the optical measurement, Digital Image Correlation (DIC) was used. With the stereoscopic setup of the Aramis system by Gesellschaft für optische Messtechnik (GOM), 3D-information can be collected. The cameras are installed at a defined angle and position according to the sample. Calibration of the system prior to the measurement is necessary to compensate the influences of radial and tangential distortions of the lenses and orientations and positions with respect to the global coordinate system of the cameras. Before the measurement, the surface of the samples has to be prepared with a high contrast stochastic surface pattern by

spray coating. The white priming coat is consisting of TiO_2 followed by a temperature-resistant black paint. The software assigns the pixels with different grey values to facets, that are recognized during different stages (e.g. different temperatures). The DIC algorithm then can calculate the surface topography and the in-plane and out-of-plane deformation.

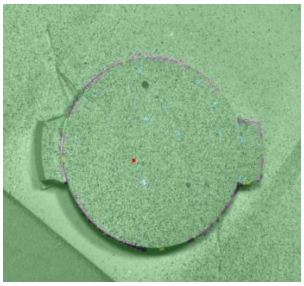

Figure 3: Prepared sensor element on spacer with black and white pattern for optical pattern recognition with DIC.

2.5 Temperature treatment and shear test measurement

To analyse the thermal shock resistance of the glass solder connection between Al_2O_3 and sapphire, cycles between 200 °C and 1000 °C are performed using an infrared oven. Test specimens are 2 mm by 2 mm alumina chips on a sapphire substrate with 9 chips per cyclization stage.
The cycle time is 7 min per cycle. This includes 2 min of heating (200 °C to 1000 °C) and 5 min of cooling from 1000 °C to 200 °C.
To analyse the interconnection quality of the glass solder, glass-soldered chips are tested in shear tests. The maximum force determined is divided by the joint area to result in the maximum shear strength. The tests were performed at room temperature and with a shear height of 300 µm.

2.6 Simulation approach

The experimental results are supported by a simulation using the finite element method. For this purpose, the material parameters found are transferred to material models. The assembly, consisting of a sapphire base plate and the glass solder connection to the Al_2O_3-spacer, are meshed in the Ansys Workbench simulation environment. The positioning in the room is carried out via a rough meshed heating plate. A temperature load of 500 °C is applied to the entire system.

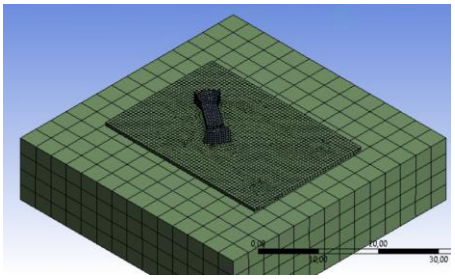

Figure 4: Finite-element-mesh for sapphire plate and glass soldered spacer on heating plate.

3 Experimental

3.1 Dilatometer measurement

The dilatometer measurement was used to determine the length change of the CTGS resonator up to a temperature of 1050 °C.

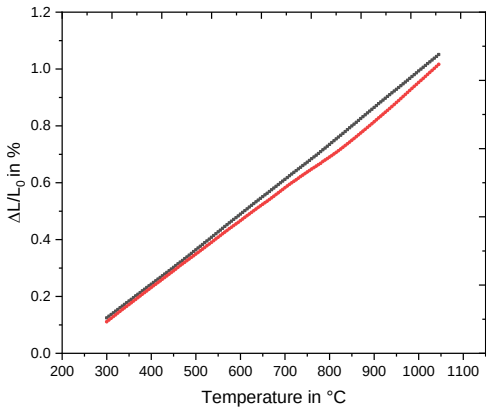

Figure 5: Dilatometer measurement of the length change of the CTGS resonator. Temperature range up to 1050 °C. Red: first temperature rise. Black: second temperature rise.

The results show a change in length of up to 1 % at a temperature of 1000 °C. For an initial length of 10 mm, this means a change of 100 µm. This is the result of free material expansion without fixing the resonator. The displacement of the resonator fixed on one side with glass solder is examined in more detail in chapter 3.3. The coefficient of thermal expansion of the CTGS material calculated from this is 8.2 ppm/K for the temperature range 300 °C to 1000 °C.

3.2 Hardness measurement CTGS

On the CTGS resonator 9 indentations are placed with equidistant spacing of 100 µm. From these a hardness value of 1150 HV is determined. According to the method of Oliver & Pharr (equation 2), an equivalent Young's modulus of 121.1 GPa could be calculated.

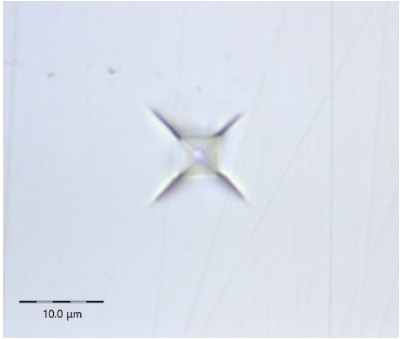

Figure 6: Indentation of the Vickers pyramid into the resonator surface of the resonator. Image taken with light microscope 100x magnification.

The picture shows a crack developing from the four corners of the indentation. This crack length can be used to determine fracture toughness of the CTGS material with formula 1.

Table 3: Determined parameters for the calculation of fracture toughness.

E (young's modulus)	121.1 GPa
H (hardness)	11.3 GPa
P (indentation force)	0.2 N
c (crack length)	4,4 µm

Using formula 1 and the values listed in table 3, a fracture toughness of 1.17 MPa·m$^{-1/2}$ can be calculated.
Pre-damage may have been introduced into the material by grinding away the platinum electrode. Compared to monocrystalline sapphire, which has a value of 2.1 MPa·m$^{-1/2}$ in [4], the value determined for monocrystalline CTGS is lower. The CTGS material is very brittle.

3.3 Optical deformation measurement of the resonator

The optical deformation measurement was able to determine the expansion of the resonator due to increased temperature up to 500 °C.

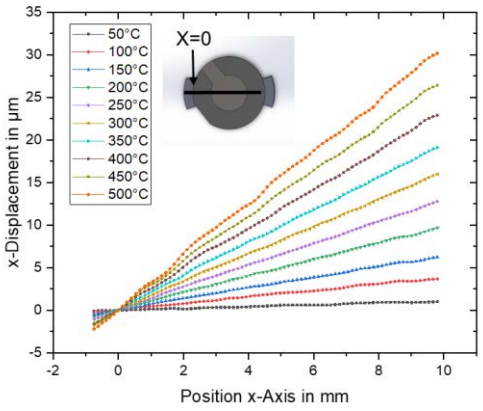

Figure 7: Deformation of the single-sided fixed resonator at temperature load up to 500 °C measured with DIC.

The measurement shows an expansion of the spacer and the resonator. The resonator is fixed to the left side of the spacer with the glass solder material presented. The spacer expands due to the temperature and thus shows the greatest change in length along the x-axis. This explains the negative values in the area to the left of x=0.
The single-sided fixed (position x=0) resonator has a total deformation of approximately 30 µm at a temperature of 500 °C. The deformation is superimposed because the sensor is fixed to the spacer. Both the spacer and the sensor show thermal expansion at 500 °C.

3.4 2θ-scan of sapphire and glass solder

X-ray diffraction enables the crystal structure of the glass solder to be analysed. The 2theta scan shows reflexes at 20.0°, 72.7°and 90.5° for the sapphire substrate. Another theta to theta scan of the sapphire wafer with a glass solder surface shows further reflections in the range around 30°, 32°, 35°, 38°, 50°, 58° and 74°. Reflections from the substrate material sapphire are visible at 20.2°, 72.7°and 90.5°

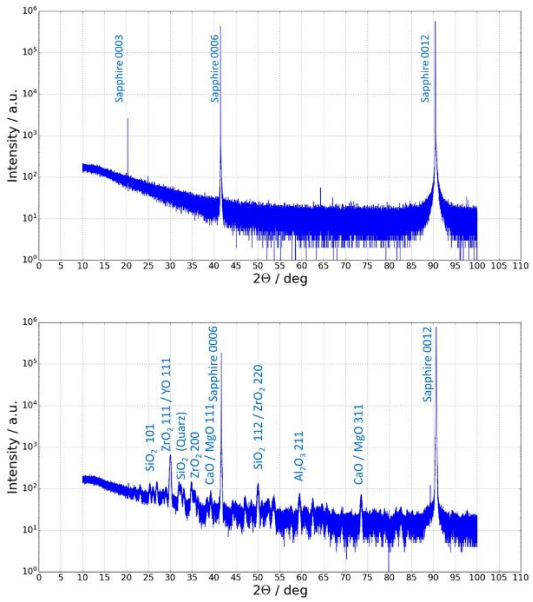

Figure 8: XRD 2theta scans. Upper sapphire scan (10° to 100°), lower glass solder (10° to 100°).

The measured secondary reflexes can be assigned to the main constituents of the glass solder (YO, SiO_2 and CaO). The YO (111) shows the largest side peak in the range of 30°. By executing a ω-2θ-scan, the incident angle ω is increased by moving the X-ray source along the goniometer circle, while the detector rotates simultaneously. Looking at the ω-2θ-scan, strongly broadened peaks can be seen, which is due to the low crystallinity of the glass solder. It can be assumed that the glass solder is in an amorphous state rather than a partially crystalline state. The other rather small side peaks like SiO_2 at 26° (101) and 50° (112) from figure 8 confirm that it is not a clear crystal orientation.

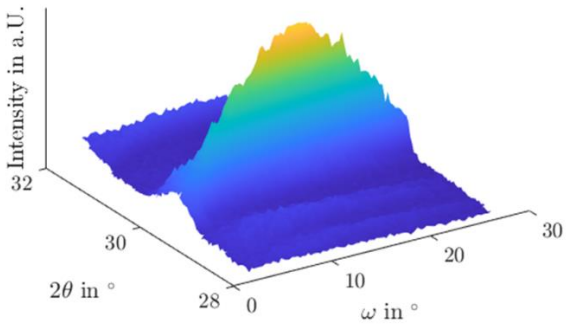

Figure 9: XRD detailed area (ω - 2θ) scan of the 30° peak. Specimen: Glass soldered surface on sapphire shown in Figure 2.

3.5 Heat treatment and shear test

The initial shear strength shows a mean value of 62,7 MPa. The mean value drops slightly to a value of 59.0 MPa after 80 temperature cycles and to a value of 57.1 MPa after 200 temperature cycles. In addition to shear strength, the cause of failure is also an important criterion. The predominant cause of failure was chip fracture or sapphire fracture. In the first 100 cycles, no failure occurred in the glass solder layer.

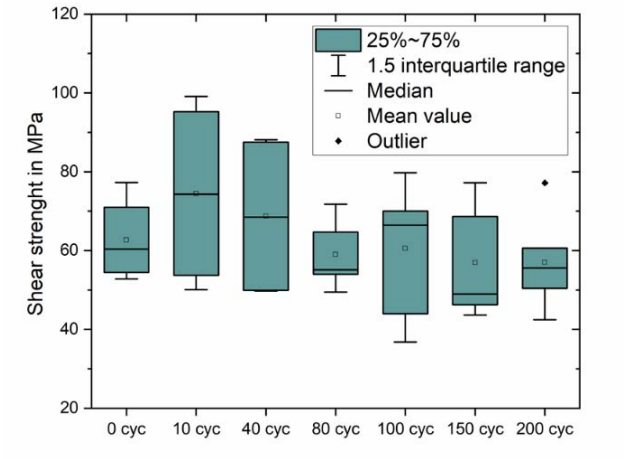

Figure 10: Influence of heat treatment 200 cycles (shock 200 °C / 1000 °C) on the shear strength of glass soldered Al_2O_3 chips, sample size n=9.

There is a stable average in shear strength even after 200 temperature cycles. After 200 cycles, 2 out of 9 chips show a failure in the glass solder connection. The main failure mechanism remains chip fracture.
It can be concluded that the glass solder connection between sapphire and alumina can withstand the thermal shock treatment and continues to show values in the range of 50 to 60 MPa in shear strength.

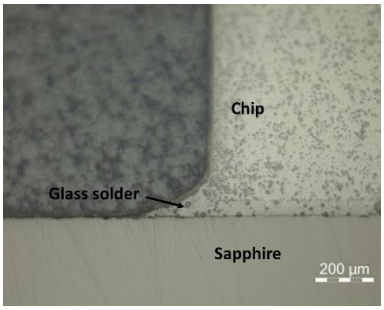

Figure 11: Cross section of a glass soldered Al_2O_3 chip after 200 cycles (200 °C / 1000 °C).

The cross-section of the glass-solder joint after 200 cycles shows no cracks in the joint layer. This confirms the results of the shear strength measurement with an almost constant curve over the 200 shock cycles between 200 and 1000 °C.

3.6 Simulation results

The results of the simulation can partially verify the measured values presented in chapter 3.3. The measured change in length of the spacer due to temperature can be confirmed by the simulation result.

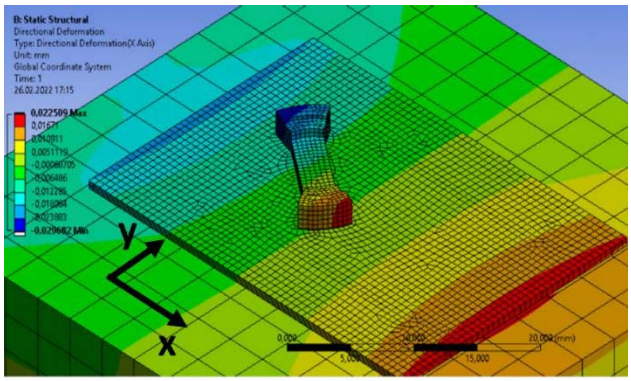

Figure 12: Deformation in x-direction of the sapphire substrate and the sensor spacer at 500 °C.

The deformation in x-direction shows a maximum value of 22 µm. In this respect, it should be noted that the x-axis is not aligned along the spacer but along the sapphire substrate. The spacer is rotated by 30° to this orientation. The amount of deformation therefore results from the sine of this angle.
The next step is the combined deformation of the spacer with the fixed resonator. Due to the additional contact condition of the resonator spacer and the point fixation by the multi-oxide glass solder material, the simulation becomes much more computationally intensive. This analysis is planned in further investigations.

4 Conclusion

This paper shows the material behaviour of ceramic assembly and interconnection technology under high temperature load. For this purpose, the thermal expansion coefficient of the CTGS sensor material was determined with a dilatometer measurement. The resistance of the material to crack propagation is analysed via the hardness measurement. The fracture toughness can be determined from the force-displacement curve of the nanoindenter measurements and the optical analysis of the indentation geometry. Furthermore, glass solder components were analysed via XRD measurement and tested for crystallinity.
The deformation of the fixed resonator was measured using optical measurement technology (DIC-system) under a temperature load up to 500 °C. The measurement shows both the linear expansion of the one-sided fixed resonator and the expansion of the spacer in the opposite direction. The temperature shock resistance of the glass solder connection could be analysed up to 200 cycles using temperature shocks. After 200 shocks, the glass-soldered joint continues to show shear strengths in the range of 50 to 60 MPa. The deformations measured via digital image correlation were confirmed via deformation simulation. It can be seen that the spacer expands longitudinally and thus exerts tension on a possibly fixed resonator.

ISBN 978-3-8007-5835-7

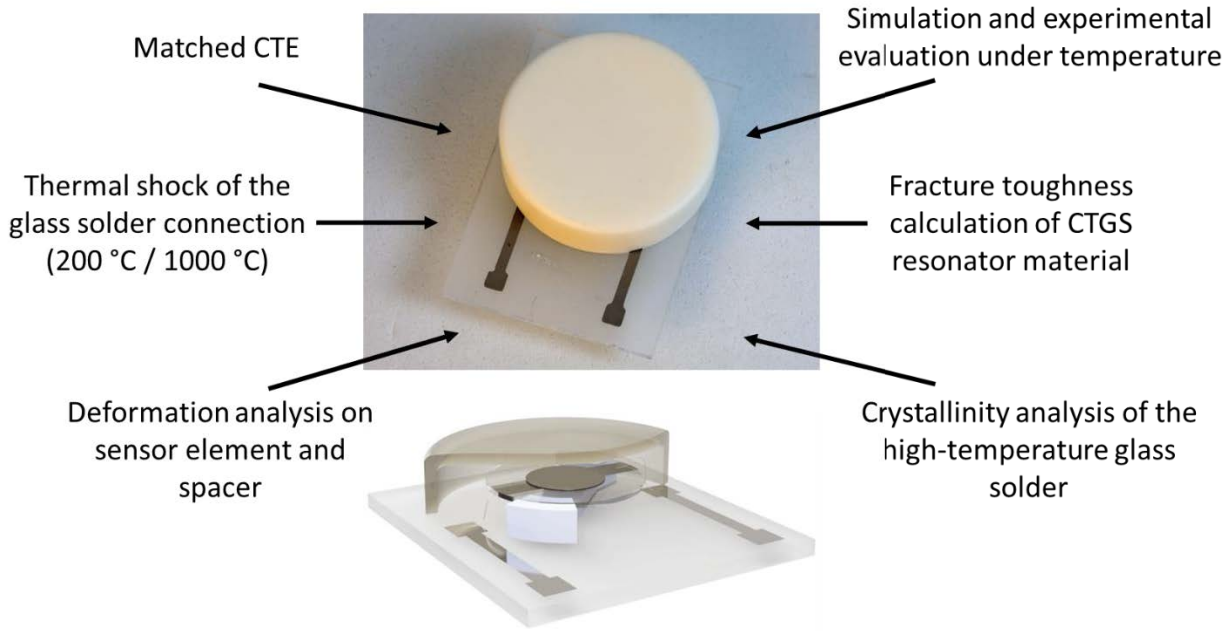

Figure 13: Investigations and analyses on the sensor model.

The investigations show a system with adjusted CTE values. The deformation analysis and simulation demonstrate the behaviour of the sensor assembly under temperature influence. The material analysis of the glass solder for crystallinity provides a precise understanding of the properties of the connection of the ceramic components.

Table 4: Characteristic sensor data at a temperature of 1000 °C. Resonator without housing and housed with the described assembly technique [7].

	Resonator alone	Resonator with housing
f_R	4.953 MHz	4.951 MHz
δf/δT	-227.8 Hz/K	-242.6 Hz/K
Q^{-1}	3.8×10^{-4}	5.6×10^{-4}
Q	2632	1786

The housing, based on sapphire, polycrystalline Al_2O_3 and glass solder, has only a limited influence on the performance parameters of the CTGS resonator like sensitivity δf/δT and quality-factor Q, table 4.
The sensor concept described represents a platform for other properties to be measured. The setup as a temperature sensor has already been functionally tested. Further setups as a pressure sensor or chemical sensor are planned.

5 Acknowledgement

The authors thank the German Research Foundation (Deutsche Forschungsgemeinschaft, DFG) for financial support under grants FR1301/35-1 and WI1987/6-1.

Many thanks also to the semiconductor characterisation group of professor Ambacher at the Department of Sustainable Systems Engineering - INATECH for their support with the XRD measurements.

6 Literature

[1] Damjanovic, D., Materials for high-temperature piezoelectric transducers, Curr. Opin. Solid State Mater. Sci. 3 (1998), 469–473.

[2] Zhao, T., Bokov, A., Wu, J., Wang, H., Wang, C., Yu, Y., Wang, C., Zeng, K., Ye, Z. and Dong, S., Giant piezoelectricity of ternary perovskite ceramics at high temperatures, Adv. Funct. Mater. 29, 2019.

[3] Segouin, V., Kaeswurm, B., Webber, K., Daniel, L., Temperature-dependent anhysteretic behavior of co-doped PZT, J. Appl. Phys. 124, 2018.

[4] Anstis G.R., Chantikul P., Lawn B.R., Marshall D.B.: A critical evaluation of indentation techniques for measuring fracture toughness: I. Direct crack measurements, JamCeramSoc 64,533-538, 1981.

[5] Marshall D.B., Lawn B.R., Evans A.G.: Elastic/plastic indentation damage in ceramics: The lateral crack system. JamCeramSoc 65, 561-571, 1982.

[6] Kohler, F., Schulz, M., Farina, M., Fritze, H., Wilde, J., Assembly and interconnection technology for high-temperature bulk acoustic wave resonators, Journal of Sensors and Sensor Systems, 2022, in press.

[7] Schulz, M., Ghanavati, R., Kohler, F., Wilde, J., Fritze, H., High-temperature behavior of housed piezoelectric resonators based on CTGS, Journal of Sensors and Sensor Systems 10, 271–279, 2021.

